# The structural and biochemical impacts of monomerizing human acetylcholinesterase

Stephanie M. Bester,[1] Kaylin A. Adipietro,[2] Vanessa L. Funk,[3] James M. Myslinski,[3] Nicholas D. Keul,[4] Jonah Cheung,[5] Paul T. Wilder,[2] Zachary A. Wood,[4] David J. Weber,[2] Jude J. Height,[3] and Scott D. Pegan ©[1,3,6]*

[1]Department of Pharmaceutical and Biomedical Sciences, University of Georgia, Athens, Georgia, 30602

[2]Department of Biochemistry and Molecular Biology, Center for Biomolecular Therapeutics, University of Maryland School of Medicine, Baltimore, Maryland, 21201

[3]U.S. Army Chemical Biological Center, Aberdeen Proving Ground, Maryland, 21010-5424

[4]Department of Biochemistry and Molecular Biology, University of Georgia, Athens, Georgia, 30602

[5]New York Structural Biology Center, New York, New York, 10027

[6]United States Research Institute of Chemical Defense, Aberdeen Proving Ground, Edgewood, Maryland

**Abstract**: Serving a critical role in neurotransmission, human acetylcholinesterase (hAChE) is the target of organophosphate nerve agents. Hence, there is an active interest in studying the mechanism of inhibition and recovery of enzymatic activity, which could lead to better countermeasures against nerve agents. As hAChE is found in different oligomeric assemblies, certain approaches to studying it have been problematic. Herein, we examine the biochemical and structural impact of monomerizing hAChE by using two mutations: L380R/F535K. The activities of monomeric hAChE L380R/F535K and dimeric hAChE were determined to be comparable utilizing a modified Ellman's assay. To investigate the influence of subunit–subunit interactions on the structure of hAChE, a 2.1 Å X-ray crystallographic structure was determined. Apart from minor shifts along the dimer interface, the overall structure of the hAChE L380R/F535K mutant is similar to that of dimeric hAChE. To probe whether the plasticity of the active site was overtly impacted by monomerizing hAChE, the kinetic constants of ($P_{R/S}$) − VX (ethyl({2-[bis (propan-2-yl)amino]ethyl}sulfanyl)(methyl)phosphinate) inhibition and subsequent rescue of hAChE L380R/F535K activity with HI-6 (1-(2′-hydroxyiminomethyl-1′-pyridinium)-3-(4′-carbamoyl-1-pyridinium))

---

were determined and found to be comparable to those of dimeric hAChE. Thus, hAChE L380R/F535K could be used as a substitute for dimeric hAChE when experimentally probing the ability of the hAChE active site to accommodate future nerve agent threats or judge the ability of new therapeutics to access the active site.

**Keywords:** acetylcholinesterase; organophosphate; nerve agent; oligomerization

## Introduction

Acetylcholinesterase (E.C. 3.1.1.7, AChE) catalyzes the hydrolysis of the neurotransmitter acetylcholine into acetate and choline, terminating its signal. AChE is located in the neuromuscular junction of all innervated organs, the autonomic ganglia, and the cholinergic synapses in the brain and spinal cord.[1] AChE exists in multiple forms including monomers, dimers, and tetramers.[2–6] These forms are distinguishable due to their oligomeric assembly and attachment modes to cell membranes.[6]

As a result of its role in the nervous system, AChE is the biological target of organophosphate (OP) nerve agents. Recent examples of the nerve agent threat include uses by Syria,[7] the ethyl({2-[bis(propan-2-yl)amino]ethyl} sulfanyl)(methyl)phosphinate (VX)-facilitated assassination of the half-brother of the North Korean leader,[8] and the use of a Novichok nerve agent in the United Kingdom.[9] Currently, the preferred treatment for OP poisoning is a combination of benzodiazepine, atropine, and the human acetylcholinesterase (hAChE) reactivator pralidoxime (2-[(hydroxyimino)methyl]-1-methylpyridin-1-ium).[10] Reactivators seek to reverse the covalent modification of hAChE's catalytic serine by OPs, which must occur prior to aging of the nerve agent–AChE complex.[11–13] The efficacy of reactivators was shown to vary based on the OP, the stereochemistry of the OP, and the species of AChE.[14–18] The flexibility of the active site, in particular the acyl loop, has recently been shown to play a role in the ability of nerve agents to inhibit hAChE and subsequent reactivation.[18,19] Although known to play a role in the inhibition and reactivation of hAChE, probing the exact influence that the plasticity of hAChE's active site has on these events has been problematic. The oligomeric size of the hAChE dimer exceeds 120 kD, limiting the effectiveness of employment of methods such as molecular dynamics (MD) and nuclear magnetic resonance (NMR).

Herein, we describe the influence of monomerization upon hAChE functionality and its ability to accommodate the nerve agent VX as well as be salvaged by a reactivator known as 1-(2′-hydroxyiminomethyl-1′-pyridinium)-3-(4′-carbamoyl-1-pyridinium), HI-6. To this end, two hydrophilic mutations L380R/F535K were introduced into the hAChE dimer interface to prevent dimer formation. The enzymatic activities of monomeric and dimeric forms of hAChE were compared. Using X-ray crystallography, a structure of hAChE L380R/F535K was obtained and compared to wild-type hAChE. Inhibition of the monomeric form of hAChE with VX and subsequent reactivation by HI-6 were evaluated and

compared to dimeric hAChE. Through these comparisons, monomeric L380R/F535K hAChE was found to have similar structural and biochemical behaviors to those of the wild-type enzyme. Hence, this opens the door to utilize the monomeric hAChE L380R/F535K in place of the hAChE dimeric form for size-sensitive studies such as modeling or MD techniques.

## Results

### Biochemical characterization of monomeric hAChE

To investigate the influence of subunit–subunit interactions on the functionality of the hAChE active site, two mutations, L380R and F535K, were engineered in order to disrupt the interface between the two hAChE subunits (PDB 4EY4). To confirm that the mutations were effective in preventing dimerization, the oligomeric states of hAChE and the hAChE L380R/F535K variant were validated through sedimentation velocity analysis (Fig. **S1**). The sedimentation coefficient for hAChE L380R/F535K was 4.03 S, which was slightly lower than the predicted value of 4.36 S. This was substantially different from 6.35 S of the hAChE, which was largely in line with the predicted value of 6.4 S. This confirmed the monomeric nature of hAChE L380R/F535K and reinforced the dimeric oligomeric state of wild-type hAChE. To investigate the impact of dimerization on the functionality of hAChE, the $K_{\mathrm{m}}$ and $k_{\mathrm{cat}}$ values of both this mutant and the dimeric hAChE were obtained side by side using a modified Ellman's assay (Table I). The $K_{\mathrm{m}}$ values of the monomeric and dimeric hAChE were consistent with one another at $8.6 \pm 1.3 \times 10^{-5}$ and $7.7 \pm 1.0 \times 10^{-5} M$, respectively. The $k_{\mathrm{cat}}$ value of the dimer of $93 \pm 3$ sec$^{-1}$ was slightly higher than that of the monomer of $70 \pm 3$ sec$^{-1}$, and these values fall within a range of percent deviation that is less than twofold difference and as such is comparable.[3,20,21] The $k_{\mathrm{cat}}$ values were determined using purified enzymes (>99%) with the enzyme concentration determined quantitatively via amino acid analyses, which is about

**Table I.** *Enzymatic Activity of Dimeric hAChE and hAChE L380R/F535K*

|  | Monomer | Dimer |
| --- | --- | --- |
| $E_{\mathrm{t}}$ (*M*) | $1.0 \times 10^{-9}$ | $9.26 \times 10^{-10}$ |
| $k_{\mathrm{cat}}$ (sec$^{-1}$) | $70 \pm 3$ | $93 \pm 3$ |
| $K_{\mathrm{m}}$ (*M*) | $8.6 \pm 1.3 \times 10^{-5}$ | $7.7 \pm 1.0 \times 10^{-5}$ |
| $V_{\mathrm{max}}$ (*M*/sec) | $6.9 \pm 0.3 \times 10^{-8}$ | $8.6 \pm 0.3 \times 10^{-8}$ |

100-fold lower than those of previous reports.[22,23] This discrepancy likely results as these studies were completed in cell culture media with enzyme concentrations calculated via antibody-based methods. This could also be due to AChE binding other components in the cell culture media (i.e., membrane), which provides the enzyme with a higher specific activity. Nonetheless, the monomerization of hAChE does not appear to affect activity as compared to dimeric hAChE.

### Structural characterization of monomeric hAChE

With the catalytic activity of the monomeric and dimeric forms of hAChE being similar, insight into the structural impact of monomerizing mutations L380R/F535K on hAChE was sought. To obtain structural information on hAChE L380R/F535K, purified protein was screened against 768 crystallization conditions. Final crystal conditions were obtained by screening pH and sodium citrate concentrations. Using crystals generated under these conditions, a 2.09 Å data set was obtained in the space group P6$_5$22, which differs from previous hAChE space groups.[18,19,24,25] Using molecular replacement with one subunit of hAChE (PDB 4EY4),[24] a solution was readily found (Table II). Unlike previous hAChE structures[18,19,24,25] that had a dimer in the asymmetric unit, hAChE L380R/F535K was a monomer. Inspection of the hAChE L380R/F535K lattice mate contacts revealed no interaction between hAChE L380R/F535K and
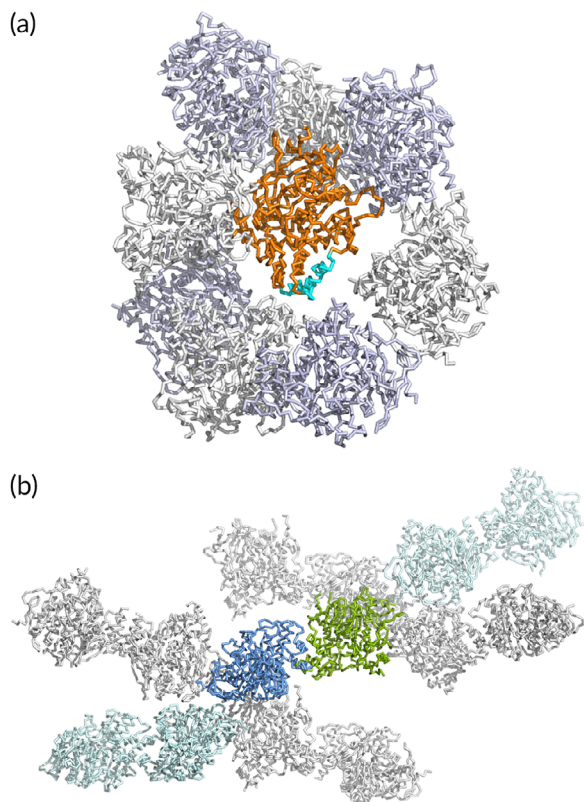


**Figure 1.** Comparison of the crystal lattice of hAChE L380R/F535K and dimeric hAChE. The asymmetric unit of the (a) monomeric (orange) (PDB 6O69) and (b) dimeric hAChE (2 subunits: baby blue, green) (PDB 4EY4) surrounded by symmetric mates (white/bluish white and light blue/light gray). The dimer interface of hAChE is depicted in aqua.

**Table II.** *Data Collection and Refinement Statistics (PDB 6O69)*

| Data collection | |
|---|---|
| Space group | P 65 2 2 |
| Cell dimensions | |
| $a, b, c$ (Å) | 115.8, 115.8, 191.9 |
| $\alpha, \beta, \gamma$ (°) | 90.0, 90.0, 120.0 |
| Resolution (Å) | 50.0–2.09 (2.13–2.09)[a] |
| Completeness (%) | 99.6 (100)[a] |
| CC1/2 | 0.977 (0.814)[a] |
| $R_{pim}$ (%) | 5.4 (32.6)[a] |
| $I/\sigma I$ | 11.1 (2.4)[a] |
| Redundancy | 12.7 (12.7)[a] |
| *Refinement* | |
| Resolution (Å) | 43.3–2.08 |
| No. of reflections | 45,954 |
| $R_{work}/R_{free}$ (%)[b] | 18.5/22.0 |
| No. of atoms | |
| Protein | 4138 |
| Ligand/ion | 38 |
| Water | 259 |
| B factors | |
| Protein | 49.4 |
| Ligand/ion | 97.7 |
| Water | 52.2 |
| RMS deviations | |
| Bond lengths (Å) | 0.015 |
| Bond angles (°) | 1.07 |

[a] Data for the last resolution shell are provided in parentheses.
[b] $R_{work}$ and $R_{free}$ = $h[|F(h)_{obs}| - |F(h)_{calc}|]/h|F(h)_{obs}|$ for reflections corresponding to the working and test sets.

its symmetry mates at the traditional hAChE dimer interface located at αF′3 and αH[26] (Fig. 1). Naturally, this contributed to hAChE L380R/F535K having a strikingly different lattice packing than previously solved structures. Hence, these findings reinforce the monomeric nature of hAChE L380R/F535K.

Globally, the monomeric hAChE L380R/F535K structure closely resembles its dimer counterpart with only a few exceptions (Fig. 2). These exceptions are largely confined to the two alpha helices that comprise the dimer interface in hAChE and contain the L380R/F535K mutations. Upon closer inspection of the region, the mutations themselves do not appear to cause a disruption to the secondary structure of either helix or the interaction between αH and αF′ helices themselves. Instead, the slight divergence of this region with that of the dimeric hAChE appears to be linked to a lack of constraints on the αH helix due to the absence of its dimeric mate. Moreover, the αH helix lacks any other crystal contacts with other monomers in the crystal lattice likely allowing it to move more freely than when part of the dimer interface. Also, the αF′3 helix is positioned closer to the core of the subunit with the lack of involvement in a dimer interface (Fig. 2). The mutations L380R/F535K themselves appear to work as designed
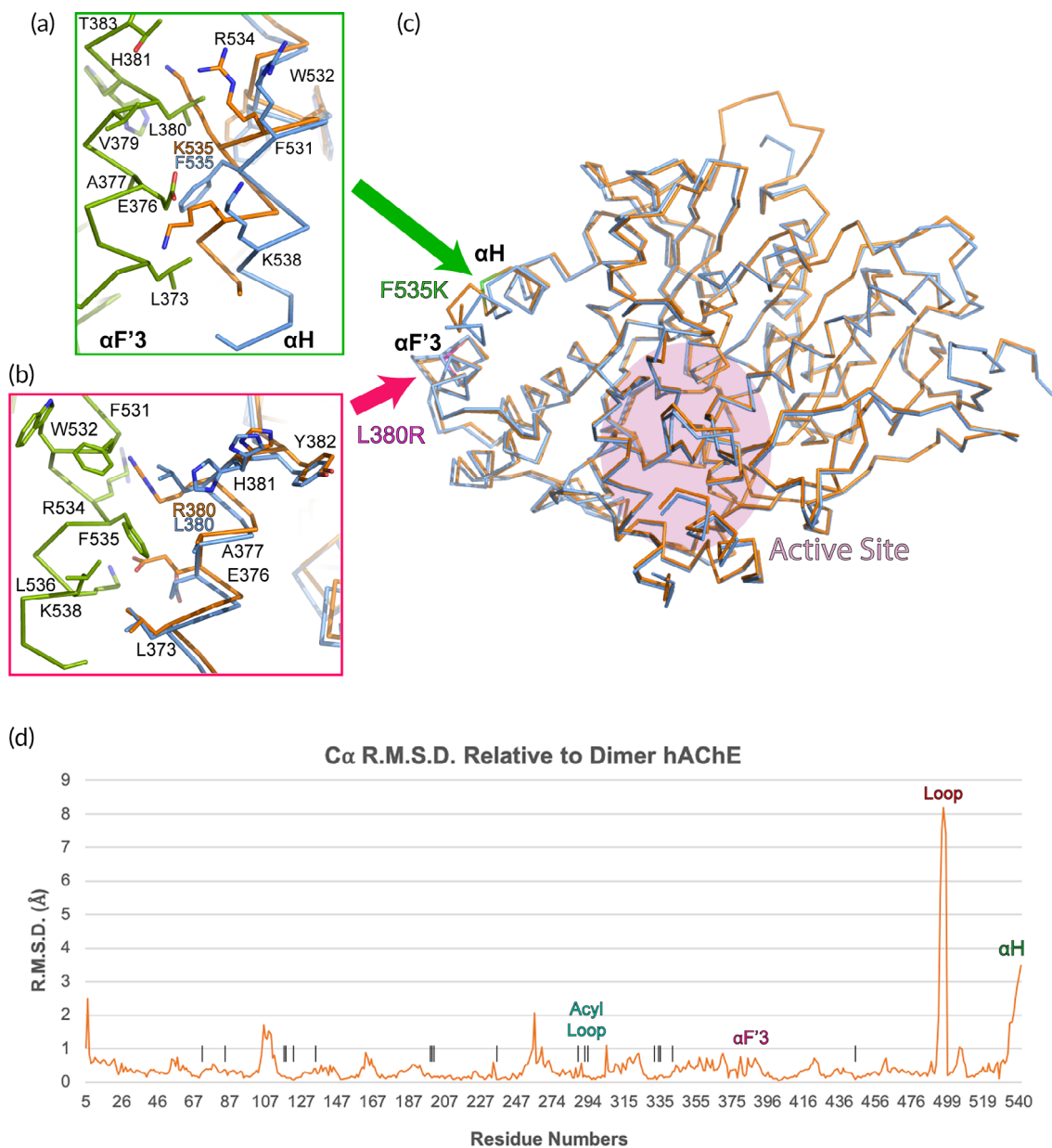
Impact of Monomerizing Human Acetylcholinesterase

**Figure 2.** Global structural comparison of monomeric hAChE L380R/F535K and dimeric hAChE. (a) Structural overlay of monomeric (orange) (PDB 6O69) and dimeric hAChE (PDB 4EY4) (2 subunits: baby blue, green). (b/c) close-up overlays of the two mutation sites on hAChE L380R/F535K compared to the dimer. The colored arrows denote the mutation sites, and the rose-colored circle indicates the active site. (d) A line graph of the root-mean-square deviation of monomeric hAChE alpha carbons when measured against dimer hAChE. αF'3 denotes the L380R mutated αF'3 helix, while αH highlights the F535K mutated αH helix. Loop and acyl loop label the 491–499 loop and acyl loop residues, respectively. The black lines emphasize the active site residues.

by turning a hydrophobic patch into one with a positive charge that is no longer sterically compatible with another subunit [Fig. 2(a,b)]. Beyond monomerizing hAChE, this also highlights the importance of the L380/F535 hydrophobic interaction on the dimer interface.

Outside the dimer interface, the presence of a loop at residues 491–499 is the most noticeable structural difference between the structures of the dimers and monomers. This loop in structures of the dimer is rarely complete and usually lacks electron density, implicating structural flexibility.[18,19,24,25] As a result, modeling of this region has been sparse. However, in

the L380R/F535K structure, residues 492–496, in particular Arg493 and Lys496, form hydrogen bonds via crystal contacts with the acyl loop and peripheral anionic site of a neighboring symmetry mate [Fig. 3 (a)]. This contact appears to have a stabilizing effect on the 491–499 loop reflected in the loop having well-defined electron density throughout, revealing at least one confirmation that the loop could adopt [Fig. 3(b)].

In contrast to the structural differences located in peripheral regions of the subunit between hAChE and its hAChE L380R/F535K monomer, the core of the enzyme is highly conserved [Fig. 2(c)]. This is
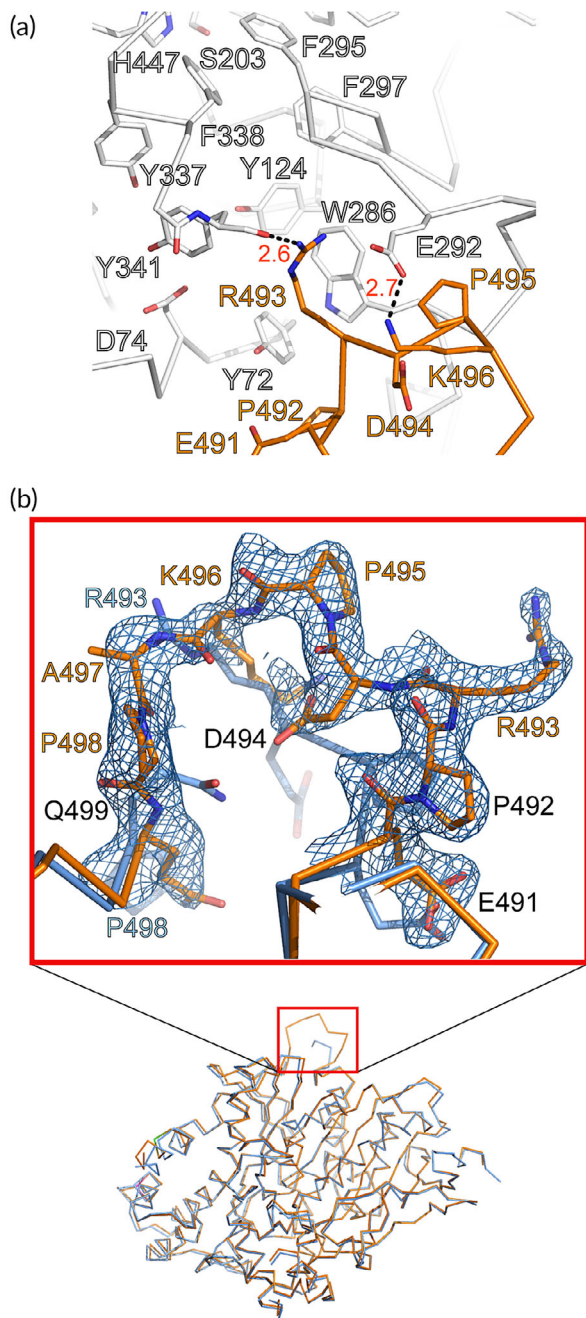
**Figure 4.** Comparison of the active sites and acyl loop of monomeric hAChE L380R/F535K and dimeric hAChE. The structures of monomeric (orange) (PDB 6O69) and dimeric hAChE (baby blue) (PDB 4EY4) are superimposed using least-squares fit of residues 176–232 of each subunit. The hAChE residues are indicated by black letters. The acyl loop is outlined with a teal dashed line and labeled in teal letters.



**Figure 3.** Comparison of the 491–499 loop of monomeric hAChE L380R/F535K and dimeric hAChE. View of $2F_o$–$F_c$ density scaled to $1\sigma$ (light blue mesh) for the 491–499 loop of the monomeric (orange) (PDB 6O69) compared to the same loop in dimeric hAChE (baby blue) (PDB 4EY4). The structures are superimposed using least-squares fit of residues 176–232 of each subunit. The black, orange, and blue letters are for labeling both, monomeric, and dimeric residues, respectively.

reflected quantitatively by the root-mean-square alpha carbon deviation of the monomeric hAChE L380R/F535K relative to hAChE [Fig. 2(d)]. Closer inspection of the hAChE active sites also supports this assertion (Fig. 4). Even the position of the highly flexible acyl loop (287–299) within the monomeric hAChE L380R/F535K structure is indistinguishable from that of the wild-type dimer.
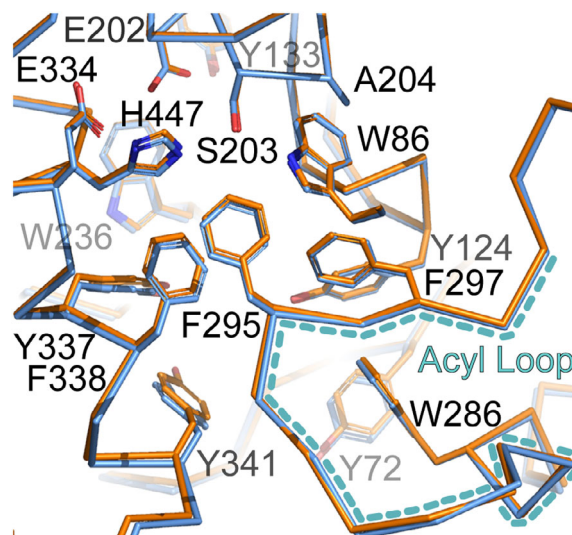
### Reactivation and inhibition of monomeric hAChE

Recently, the plasticity within the active site of hAChE has been implicated in the ability of the enzyme to be inhibited by nerve agents and rescued by reactivating agents.[18,19] To explore whether the flexibility of the active site was overly impacted by the monomerization of hAChE by the mutations L380R/F535K, the kinetic constants of $(P_{R/S})$ – VX inhibition and subsequent rescue by HI-6 were obtained. The determined dissociation constant, $K_d$, and the unimolecular bonding rate constant, $k_2$, of hAChE L380R/F535K are slightly different from the values previously recorded for dimeric hAChE; however, the yielded bimolecular rate constant, $k_i$, of $7.9 \times 10^7\,M^{-1}\,min^{-1}$ for $(P_{R/S})$ – VX-inhibited hAChE L380R/F535K is consistent with the $k_i$ value of dimeric hAChE from previous studies (Tables III and IV).[18] As the potency of $(P_{R/S})$ – VX appeared consistent for both enzymes, a modified Ellman's assay was utilized to assess the ability of HI-6 to reactivate $(P_{R/S})$ – VX inhibited monomeric hAChE L380R/F535K. The $k_r$ value of HI-6 for monomeric hAChE inhibited by $(P_{R/S})$ – VX was revealed to be $0.02 \pm 0.01\,\mu M^{-1}\,min^{-1}$. When compared to previous studies, this fits the general trend observed for HI-6 reactivation of $(P_{R/S})$ – VX-inhibited dimeric hAChE.[15,17,18]

### Discussion

#### Role of dimerization in hAChE

In nature, AChE has been found in various oligomeric states among vertebrate species.[6,27] Given the various oligomeric forms of AChE, there has been an

Impact of Monomerizing Human Acetylcholinesterase

**Table III.** *Inhibition of hAChE*

| hAChE | OP | $k_2$ (min$^{-1}$) | $K_d$ (M) | $k_i$ (M$^{-1}$ min$^{-1}$) |
|---|---|---|---|---|
| Monomer | (P$_{R/S}$) – VX | $2.2 \times 10^{-1}$ | $2.9 \times 10^{-9}$ | $7.9 \times 10^7$ |
| Dimer[a] | (P$_{R/S}$) – VX | $4.5 \times 10^{-2}$ | $5.9 \times 10^{-10}$ | $7.7 \times 10^7$ |

[a] From Ref. 18.

**Table IV.** *Reactivation of Inhibited hAChE by HI-6*

| | | $k_2$ (min$^{-1}$) | $K_{OX}$ (μM) | $k_r$ (μM$^{-1}$ min$^{-1}$) | max% |
|---|---|---|---|---|---|
| Monomer | (P$_{R/S}$) – VX | $0.30 \pm 0.08$ | $19.9 \pm 7.0$ | $0.02 \pm 0.01$ | >100 |
| Dimer[a] | (P$_{R/S}$) – VX | $0.63 \pm 0.04$ | $7.50 \pm 2.1$ | $0.08 \pm 0.02$ | >100 |
| Dimer[a] | (P$_S$) – VX | $0.71 \pm 0.06$ | $23.3 \pm 8.0$ | $0.03 \pm 0.01$ | 92 |

[a] From Ref. 18.

interest in whether cooperativity exists for this class of enzymes. Binding of AChE ligands, such as fasciculin-2, at peripheral sites has been suggested to induce allosteric intrasubunit effects on the independent catalytic sites.[28,29] However, in general, there is no evidence for subunit cooperativity in hAChE based on its substrates.[30] Although the lack of communication between the subunits of hAChE is well documented, information on whether the dimer interface itself influences the behavior of the enzyme has largely been limited to *in silico* modeling of the MD of hAChE related to oligomerization. For example, Gorfe et al. determined that despite steric effects arising from oligomerization of hAChE, enzymatic efficiency between different oligomeric states was maintained due to favorable electrostatic interactions.[31] In our work, the monomerization of hAChE through dimer interface disrupting mutations L380R/F535K allowed an initial glance into the effect of the dimer interface upon the enzyme's structural and biochemical behavior. As demonstrated, the monomeric hAChE L380R/F535K behaves biochemically similar to that of its dimeric wild-type form. Similar kinetics along with the structural similarities of the active site of hAChE L380R/F535K and wild-type hAChE reinforce the notion that interactions along the dimer interface do not impact the functionality of hAChE appreciably. Thus, the oligomerization of hAChE is likely driven by other biological factors, such as the spatial and temporal demands of specific synapses.[27]

### Monomeric hAChE as a tool for the development of nerve agent therapeutics

As several nations have rushed to develop nerve agents that target hAChE, acetylcholine has not been the only ligand of scientific interest when it comes to this enzyme.[32] The hAChE active site did not evolve to process these OP agents that at times appear to be ill-fitting to the active site. Not surprisingly, recent reports have tied the plasticity of the active site, particularly that of the acyl loop, as playing a role in the ability of nerve agents to inhibit the enzyme as well as therapeutic agents salvaging it.[18,19] Although X-ray crystal structures of hAChE

have provided insight into the role that plasticity can play regarding nerve agents and current therapeutics, the ability to measure the actual flexibility of the active site has been limited. Additionally, the ability to simulate or model the behavior of these compounds including their exit and entry into the active site would be immensely beneficial for the development of new reactivators and other therapeutics. MD techniques as well as NMR are potential methods to resolve some of these lingering questions. However, the size of the studied protein can be a major complication in utilizing many of these techniques to the point of being impossible.[33] For instance, NMR is an excellent technique for obtaining dynamic information for different regions and domains of a protein including protein flexibility. However, it is generally extremely challenging for proteins exceeding 70 kDa unless the system being studied has unique properties.[34,35] Additionally, larger macromolecules can affect the root-mean-square deviation (RMSD) of structures or atomic coordinates, a measure of similarity that is often used to analyze MD trajectories, modeling, and docking.[36–39] MD simulations run on larger macromolecules can result in the RMSD losing the ability to discriminate conformation differences between structures and dynamics.[33]

As the subunit molecular weight of this recombinant hAChE is ~60 kDa, dimeric and tetrameric forms of hAChE pose problems for these NMR or MD approaches. The monomerization of hAChE through selective mutagenesis at L380R/F535K appears to offer a new way around these size constraints. Not only is the hAChE L380R/F535K active site structurally indistinguishable from that of wild type, but it mirrors the wild-type hAChE performance with regard to acetylcholine. Even for large nerve agents such as VX and reactivating agents like HI-6 that require additional plasticity of the active site, hAChE L380R/F535K reacts similarly to wild-type hAChE. Thus, the monomeric hAChE L380R/F535K could be used as a stand in for the dimer, or even tetrameric hAChE in NMR and MD studies. This would facilitate experimentally probing the ability of the hAChE

active site to accommodate future nerve agent threats like those of A-series agents or judge the ability of new therapeutics *in silico* to access the active site to counter them.

## Material and Methods

### Materials

Bovine serum albumin (BSA) was purchased from VWR International (Radnor, PA), while acetylthiocholine iodide (ATCI), sodium citrate, sodium chloride, potassium chloride, sodium carbonate, monosodium phosphate, and disodium phosphate were purchased from Sigma-Aldrich (St. Louis, MO). 2-[4-(2-hydroxyethyl) piperazin-1-yl]ethanesulfonic acid (HEPES) was purchased from Hampton Research. Hexanes, 5,5′-dithiobis (2-nitrobenzoic acid) (DTNB), and isopropyl alcohol were purchased from Thermo Fisher Scientific (Waltham, MA). Laboratory deionized water of >17 MΩ was used for all assays.

### Cloning, expression, and purification of hAChE

The GeneArt Site-Directed Mutagenesis System (Thermo Fisher Scientific) was used to introduce site-directed amino acid substitutions of L380R/F535K into the hAChE sequence of the pJTI Fast Dest hAChE vector using PCR-based methods.[24] Cloning, expression, and purification of mutant and dimeric hAChE were adapted from a previous study[24] by inserting the octahistidine (His8) tag followed by ENLYFQ after residue 32 at the N terminus to form a complete ENLYFQG TEV protease site with G33 of the native hAChE sequence and transfecting the recombinant hAChE mutant amino acid sequence 1–574 (preprocessed protein numbering that includes the native secretion signal) encoded construct into FreeStyle 293-F Cells (ThermoFisher Scientific). Purified protein was dialyzed into storage buffer (10 m$M$ HEPES, pH 7.0, and 10 m$M$ NaCl) overnight and then concentrated to desired concentrations.

### Sedimentation velocity

Monomeric hAChE (11 μ$M$) was dialyzed into 50 m$M$ HEPES pH 7.5 and 150 m$M$ KCl) and loaded into an equilibrated cell equipped with 12 mm double-sector Epon centerpieces and quartz windows. Sedimentation velocity data were collected using an Optima XLA analytical ultracentrifuge at 50,000 rpm for 8 hr. SEDNTERP[40] was used to estimate the partial specific volume of monomeric AChE (0.73248 mL/g) and the density (1.00726 g/mL) and viscosity (0.01018 P) of the buffer. Data were modeled as a continuous sedimentation coefficient ($c[s]$) distribution using SEDFIT.[41] The following parameters were fit during data modeling: baseline, meniscus, frictional coefficient, and systematic time-invariant and radial-invariant noise.[42] The fit data had an RMSD of 0.006579 AU. Dimeric hAChE (10 μ$M$) was diluted with 10 m$M$ HEPES and 10 m$M$ NaCl at pH 7.4–1 μ$M$. The sedimentation velocity experiment was run at 20°C in a Beckman XL-I analytical ultracentrifuge using an An-60 Ti rotor. HYDROPRO[43] was used to predict the $s$ values of both monomeric and dimeric hAChE based on atomic coordinates (PDB: 6O69; PDB 4EY4).

### Enzymatic characterization of monomeric and dimeric hAChE

Equivalent concentrations of purified dimeric and monomeric AChE subunits were added to a 96-well plate and used in a modified Ellman's assay (final volume: 250 μL) at 25°C. Each well contained a final concentration of 0.1$M$ phosphate buffer at pH 8.0 with 0.1 mg/mL BSA at pH 8.0, 0.3 m$M$ DTNB, and increasing amounts of ATCI (0–1.5 m$M$) that was added immediately before analysis. The assay plate was read using a PHERAstar FS (BMG Labtech) at an absorbance of 412 nm with path length correction on every 20 sec for 20 min. The $K_m$, $V_{max}$, and $k_{cat}$ values were determined using the equation $V_{max} = k_{cat} \times [E_t]$, where $E_t$ is the total enzyme concentration ($M$), as determined using quantitative amino acid analyses (Bio-Synthesis, Inc.). Data were plotted using GraphPad Prism.

### X-ray structure determination of hAChE mutant L380R/F535K

The hAChE L380R/F535K (16 mg/mL) was screened against eight Qiagen NeXtal suites in a hanging drop format with a TTP LabTech Mosquito (TTP Labtech, Herfordshire, UK). The final crystals were obtained by hanging drop vapor diffusion at 22°C against 500 μL of crystallization buffer. Crystals were subsequently placed in crystallization buffer with 20% of a 1:1:1 solution of ethylene glycol, dimethyl sulfoxide, and glycerol[44] as a cryoprotectant before being mounted onto liquid nitrogen flash-cooled nylon loops. A data set was collected for monomeric AChE with a resolution of 2.09 Å on the 22ID beamline of Southeast Regional Collaborative Access Team (SERCAT) at a wavelength of 1 Å at the Advanced Photon Source, Argonne National Laboratory, with a monochromic X-ray beam using a Dectris Eiger 16M PIXEL detector. The data collection, reduction, and refinement occurred as previously described.[18] To verify the structure's quality, the final model was analyzed via MolProbity. The data collection and refinement statistics for the structure are provided in Table II (PDB 6O69).

### Measurement of inhibition and reactivation rate constants

All procedures with regard to measurement of inhibition and reactivation rate constants of L380R/F535K (monomer) hAChE were adapted from a previous study.[18] To determine the inhibition rate constants, modified Ellman's assays were run with a quantity of hAChE, equivalent to 3–4 U/mL of activity, with varying concentrations of ($P_{R/S}$) – VX (0.38, 0.34, 0.25, 0.17, 0.12, and 0 μ$M$), DTNB (0.3 m$M$), and acetylthiocholine (ATC) (1 m$M$) (final volume: 250 μL). The method used

to calculate inhibition rate constants was a continuous method.[45] The procedures and calculations utilized to determine the reactivation rate constants of hAChE L380R/F535K were modified from a previous study where $k_2$ is the intrinsic reaction constant; $K_{OX}$ is the apparent equilibrium constant; and $k_r$ is the second-order reactivation rate constant.[18] Reactivation of inhibited hAChE was established by adding the reactivator (HI-6) (1250, 312.5, 187.5, 18.75, and 1.875 μ$M$ and at final concentration) to inhibited hAChE followed by DTNB and ATC. The activities were measured at 30 sec and 1, 2, 3, 4, 5, and 30 min.

## Acknowledgments

## Author Contributions

The manuscript was written through contributions of all authors. All authors have given approval to the final version of the manuscript.

## Data Availability Statement

The atomic coordinates and structural factors (code 6O69) was deposited in the RCSB Protein Data Bank, www.rcsb.org.

## References

1. Eddleston M (2000) Patterns and problems of deliberate self-poisoning in the developing world. QJM 93:715–731.
2. Bon S, Massoulie J (1976) An active monomeric form of *Electrophorus electricus* acetylcholinesterase. FEBS Lett 67:99–103.
3. Gordon MA, Carpenter DE, Wilson IB (1978) The turnover numbers of acetylcholinesterase forms. Mol Pharmacol 14:266–270.
4. Vigny M, Bon S, Massoulie J, Leterrier F (1978) Active-site catalytic efficiency of acetylcholinesterase molecular forms in electrophorus, torpedo, rat and chicken. Eur J Biochem 85:317–323.
5. Barnett P, Rosenberry TL (1979) Functional identity of catalytic subunits of acetylcholinesterase. Biochim Biophys Acta 567:154–160.
6. Massoulie J, Bon S (1982) The molecular-forms of cholinesterase and acetylcholinesterase in vertebrates. Annu Rev Neurosci 5:57–106.
7. Kingsley P, Barnard A (2017) Banned nerve agent sarin used in Syria chemical attack, Turkey says. The New York Times.
8. Paddock R, Sang-Hun C, Wade N (2017) In Kim Jong-nam's death, North Korea lets loose a weapon of mass destruction. The New York Times.
9. Barry E, Yeginsu C (2018) The nerve agent too deadly to use, until someone did. The New York Times.
10. Buckley NA, Roberts D, Eddleston M (2004) Overcoming apathy in research on organophosphate poisoning. BMJ 329:1231–1233.
11. Hobbiger F (1957) Reactivation of phosphorylated acetocholinesterase by pyridine-2-aldoxime methiodide. Biochim Biophys Acta 25:652–654.
12. Simeon V, Skrinjaric-Spoljar M, Wilhelm K (1973) Reactivation of phosphorylated cholinesterases in vitro and protecting effects in vivo of some pyridinium and quinolinium oximes. Arh Hig Rada Toksikol 24:11–18.
13. Sun M, Chang Z, Shau M, Huang R, Chou T (1979) The mechanism of ageing of phosphonylated acetylcholinesterase. Eur J Biochem 100:527–530.
14. Worek F, Reiter G, Eyer P, Szinicz L (2002) Reactivation kinetics of acetylcholinesterase from different species inhibited by highly toxic organophosphates. Arch Toxicol 76:523–529.
15. Worek F, Thiermann H, Szinicz L, Eyer P (2004) Kinetic analysis of interactions between human acetylcholinesterase, structurally different organophosphorus compounds and oximes. Biochem Pharmacol 68:2237–2248.
16. Maxwell DM, Koplovitz I, Worek F, Sweeney RE (2008) A structure-activity analysis of the variation in oxime efficacy against nerve agents. Toxicol Appl Pharmacol 231:157–164.
17. Reiter G, Muller S, Hill I, Weatherby K, Thiermann H, Worek F, Mikler J (2015) In vitro and in vivo toxicological studies of V nerve agents: molecular and stereoselective aspects. Toxicol Lett 232:438–448.
18. Bester SM, Guelta MA, Cheung J, Winemiller MD, Bae SY, Myslinski J, Pegan SD, Height JJ (2018) Structural insights of stereospecific inhibition of human acetylcholinesterase by VX and subsequent reactivation by HI-6. Chem Res Toxicol 31:1405–1417.
19. Franklin MC, Rudolph MJ, Ginter C, Cassidy MS, Cheung J (2016) Structures of paraoxon-inhibited human acetylcholinesterase reveal perturbations of the acyl loop and the dimer interface. Proteins 84:1246–1256.
20. Quinn DM (1987) Acetylcholinesterase - enzyme structure, reaction dynamics, and virtual transition-states. Chem Rev 87:955–979.
21. Hsieh JY, Chen SH, Hung HC (2009) Functional roles of the tetramer organization of malic enzyme. J Biol Chem 284:18096–18105.
22. Shafferman A, Velan B, Ordentlich A, Kronman C, Grosfeld H, Leitner M, Flashner Y, Cohen S, Barak D, Ariel N (1992) Substrate inhibition of acetylcholinesterase: residues affecting signal transduction from the surface to the catalytic center. EMBO J 11:3561–3568.
23. Masson P, Schopfer LM, Bartels CF, Froment MT, Ribes F, Nachon F, Lockridge O (2002) Substrate activation in acetylcholinesterase induced by low pH or mutation in the pi-cation subsite. Biochim Biophys Acta 1594:313–324.
24. Cheung J, Rudolph MJ, Burshteyn F, Cassidy MS, Gary EN, Love J, Franklin MC, Height JJ (2012) Structures of human acetylcholinesterase in complex with pharmacologically important ligands. J Med Chem 55:10282–10286.
25. Allgardsson A, Berg L, Akfur C, Hornberg A, Worek F, Linusson A, Ekstrom FJ (2016) Structure of a prereaction complex between the nerve agent sarin, its biological target acetylcholinesterase, and the antidote HI-6. Proc Natl Acad Sci U S A 113:5514–5519.
26. Sussman JL, Harel M, Frolow F, Oefner C, Goldman A, Toker L, Silman I (1991) Atomic structure of acetylcholinesterase from *Torpedo californica*: a prototypic acetylcholine-binding protein. Science 253:872–879.
27. Massoulie J, Pezzementi L, Bon S, Krejci E, Vallette FM (1993) Molecular and cellular biology of cholinesterases. Prog Neurobiol 41:31–91.
28. Radic Z, Quinn DM, Vellom DC, Camp S, Taylor P (1995) Allosteric control of acetylcholinesterase catalysis by fasciculin. J Biol Chem 270:20391–20399.

29. Johnson G, Moore SW (2006) The peripheral anionic site of acetylcholinesterase: structure, functions and potential role in rational drug design. Curr Pharm Des 12: 217–225.

30. Meister A. Acetylcholinesterase. (1975) Advances in enzymology and related areas of molecular biology. New York: John Wiley and Sons, Inc., pp 103–218.

31. Gorfe AA, Lu B, Yu Z, McCammon JA (2009) Enzymatic activity versus structural dynamics: the case of acetylcholinesterase tetramer. Biophys J 97:897–905.

32. Newmark J. Chapter 56 - nerve agents. In: Dobbs MR, Ed., 2009, Clinical neurotoxicology. Philadelphia: W.B. Saunders; p. 646–659.

33. Sargsyan K, Grauffel C, Lim C (2017) How molecular size impacts RMSD applications in molecular dynamics simulations. J Chem Theory Comput 13:1518–1524.

34. Berjanskii M, Wishart DS (2006) NMR: prediction of protein flexibility. Nat Protoc 1:683–688.

35. Kristensen SM, Kasimova MR, Led JJ. The use of NMR in the studies of highly flexible states of proteins: relation to protein function and stability. In: Webb GA, Ed. , 2006Modern magnetic resonance. Dordrecht: Springer Netherlands; p. 1369–1376.

36. Shoichet BK, Kuntz ID (1991) Protein docking and complementarity. J Mol Biol 221:327–346.

37. Kozakov D, Clodfelter KH, Vajda S, Camacho CJ (2005) Optimal clustering for detecting near-native conformations in protein docking. Biophys J 89:867–875.

38. Mukherjee S, Balius TE, Rizzo RC (2010) Docking validation resources: protein family and ligand flexibility experiments. J Chem Inf Model 50:1986–2000.

39. Schuetz DA, Bernetti M, Bertazzo M, Musil D, Eggenweiler HM, Recanatini M, Masetti M, Ecker GF, Cavalli A (2019) Predicting residence time and drug unbinding pathway through scaled molecular dynamics. J Chem Inf Model 59:535–549.

40. Laue TM, Shah BD, Ridgeway TM, Pelletier SL. Analytical ultracentrifugation. Cambridge: The Royal Society of Chemistry, 1992.

41. Schuck P (2000) Size-distribution analysis of macromolecules by sedimentation velocity ultracentrifugation and Lamm equation modeling. Biophys J 78:1606–1619.

42. Schuck P (2003) On the analysis of protein self-association by sedimentation velocity analytical ultracentrifugation. Anal Biochem 320:104–124.

43. Ortega A, Amoros D, Garcia de la Torre J (2011) Prediction of hydrodynamic and other solution properties of rigid proteins from atomic- and residue-level models. Biophys J 101:892–898.

44. Sanchez JE, Gross PG, Goetze RW, Walsh RM, Peeples WB, Wood ZA (2015) Evidence of kinetic cooperativity in dimeric ketopantoate reductase from *Staphylococcus aureus*. Biochemistry 54:3360–3369.

45. Forsberg A, Puu G (1984) Kinetics for the inhibition of acetylcholinesterase from the electric eel by some organophosphates and carbamates. Eur J Biochem 140:153–156.

Impact of Monomerizing Human Acetylcholinesterase